研究論文

# Study on Flow Field and Heat Transfer Characteristics of Heat Sinks with Continuous, Offset Strip, or Pin Fins Cooled by Laminar Duct Flow

Jun SUZUKI*1 Himsar AMBARITA*1 Koki KISHINAMI*1 Mashashi DAIMARUYA*1 Hideki KAWAI*1

## Abstract

The present paper deals with numerical study on flow field and heat transfer characteristics of heat sinks with continuous, offset strip, or pin fins. The heat sinks were made of aluminum alloy, originally, consists of six identical continuous plates. Then, each plate is divided into $n$ number of identical strip fins by cutting off some fins material. Hence, total heat transfer area (wetted area) of the heat sinks was fixed. The strip fins were arranged in staggered positions. The fin number, $n$, was varied from 1 (referred as continuous fins), $n$=4, 8, 16, 20 (strip fins), and $n$=25, 29 (pin fins). The heat sinks were cooled by forced convection of ambient air in a duct. Base temperature of the heat sinks was $50^0$C, ambient air was $20^0$C, and inlet velocity was varied from 0.5, 1, 2, and 3 m/s. Three-dimensional, steady state, and laminar of the governing equations were solved based on finite volume method. Flow and temperature fields, heat transfer coefficient, total heat transfer rate as a function of inlet velocity were presented. The results show that using offset strip fins, instead of continuous fins, does enhance the heat transfer rate. However, in comparison with less fin number, attaching too many fin number will decrease the heat transfer rate. This is because the cross-sectional area of the fins becomes smaller, the presence of the reversal flow becomes significant, and number of fins in fully developed flow region becomes larger. It is also shown that there exists an optimum fin number for maximum heat transfer rate. The optimum fin number of the present heat sinks was 20. By using this fin number, the heat transfer rate at inlet velocity 3 m/s will be enhanced up to 214 percent and fins material will be reduced up to 66.6 percent in comparison to the heat sink with continuous fins.

Keywords: Heat sink, Continuous fin, Offset strip fin, Pin fin

## 1. Introduction

Heat sink is an object which absorbs and dissipates excess heat from another object or environment. It is used in many engineering applications. Noticeable examples included cooling of electronic devices, such as in a personal computer, and electro-luminescence board. The heat sink is generally cooled by forced convection of ambient air. It is realized that the heat transfer coefficient of the air is very weak. In order to solve this weakness, extended surface area and/or heat transfer enhancement techniques are commonly used. To provide the extended surface area, heat sinks with parallel plate (continuous fins) have been widely used due to its simplicity. Thus, study on the forced convection of the heat sinks with continuous fins have been extensively conducted up to now [1-2]. It is well known that the heat transfer coefficient at the entrance region of a plate cooled by a stream is substantially larger than that at locations farther downstream in fully developed region. Hence, in order to provide both extended surface area and heat transfer enhancement effects, offset strip and pin fins have been widely used [3-9]. A brief literature review has been made and it shows that most of those papers focused on the effects of the cross-sections of the fins, such as circular, elliptic, and NACA fins.

When a continuous fin is divided into a moderate fin number, it becomes a number of strip fins. If they are arranged in staggered position and cooled at the same operational condition, total heat transfer coefficient of the offset strip fins will be better than the continuous fin. This is because the presence of acceleration flows and fully developed prevention provided by offset strip fins. Thus, using a number of strip fins, instead of continuous fin, will significantly enhance the heat transfer rate. However, if the continuous fin is divided into an extremely big fin number, it becomes pin fins due to the cross-sectional area of the strip fins becomes very small. Hence, the pin

*1 Dept. of Mechanical System Engineering, Muroran Institute of Technology, Muroran-shi Mizumoto cho 27-1, 050-8585 Hokkaido, JAPAN, email: himsar@gmail.com
*Corresponding author: himsar@gmail.com
（原稿受付：2007年8月7日）

fins become less effective due to their thermal conductivity is not infinity. In addition, the presence of the reversal flows behind the pin fins will be significant and it will affect the total heat transfer rate. Consequently, in comparison with a moderate fin number, using too many fin number will not enhance the heat transfer rate. Based on this fact there must exists an optimum fin number per row for maximum heat transfer rate.

The present paper will study on flow field and heat transfer characteristics of heat sinks with continuous, offset strip, or pin fins cooled by forced convection of laminar duct flow. The main objective is to prove and to seek the optimum fin number per row for maximum heat transfer rate of the considered heat sinks. None of those papers cited above [1-9] has explored the optimum fin number per row in a heat sink. In order to solve this problem numerical simulations have been carried out.

## 2. Problem Definition

The model of the heat sinks and its dimensions are adopted from heat sinks used in electro-luminescence boards of Shinyo-sha L.T.D, Tokyo Japan. The considered heat sink is depicted in Fig.1. It was made of aluminum alloy with a thermal conductivity of 170 $Wm^{-1}K^{-1}$ and density 2787 $kgm^{-3}$. Dimensions of the heat sink are $W$=48 mm, length $Ls$=114 mm and $H_f$= 20 mm. The clearance of the heat sink to the roof of the duct is 5 mm. The heat sink, originally, consists of six parallel continuous plates with thickness $d$ =2 mm. The clearance between plates is 3$d$. Then, each plate was divided into $n$ number of strip fins and they were arranged in staggered positions. The fin number was varied $n$ =1, 4, 8, 16, 20, 25, and 29. To make convenient discussions, the heat sinks are named as model HS1, HS4, HS8, HS16, HS20, HS25, and HS29, respectively. Based on the strip fin's length, the heat sinks can be divided into three types: continuous fins (HS1), strip fins (HS4, HS8, HS16, and HS20), and pin fins (HS25 and HS29). In order to make the fair comparison, total heat transfer areas (wetted areas) are fixed. To keep a fixed heat transfer area, a gap (=$d$) was attached between strip/pin fins by cutting off some fins material.

The heat sinks were cooled in a duct by forced convection of ambient air. Thermal properties of the ambient air are as follows. Density, specific heat, viscosity, and thermal conductivity are: 1.293 $kgm^{-3}$, 1.006 $kJkg^{-1}$, $1.76\times10^{-5}$ $kgs^{-1}m$, and 0.025 $Wm^{-1}K^{-1}$, respectively. Detailed fins dimensions of the heat sinks are presented in Table 1.

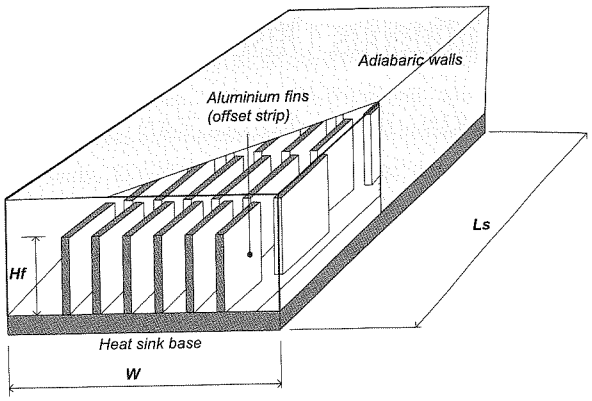


Fig. 1 Offset strip fins type of considered heat sink.

Data of the table show that total surface area of the fins decreases with increases of the fin number, $n$. This is because the presence of the extended surfaces from both front and rear surfaces of the fins. The base area of the heat sink increases with increases of the fin number. However, the total heat transfer areas (wetted areas) are fixed. As a matter of fact, the table shows that total mass of the fins material decreases as fin number increases.

Table 1 Detailed fins dimensions of the heat sinks

| Model | $n$ | $L$ [mm] | $A_f$ [$mm^2$] | $A_b$ [$mm^2$] | $A_{tot}$ [$mm^2$] | $m_f$ [gr.] |
|---|---|---|---|---|---|---|
| HS1 | 1 | 114 | 29208 | 4104 | 33312 | 76.25 |
| HS4 | 4 | 27 | 29136 | 4176 | 33312 | 72.24 |
| HS8 | 8 | 12.5 | 29040 | 4272 | 33312 | 66.89 |
| HS16 | 18 | 5.25 | 28848 | 4464 | 33312 | 56.19 |
| HS20 | 20 | 3.28 | 28752 | 4560 | 33312 | 50.83 |
| HS25 | 25 | 2.64 | 28632 | 4680 | 33312 | 44.15 |
| HS29 | 29 | 2.0 | 28536 | 4776 | 33312 | 38.79 |

## 3. Numerical procedure

In order to reduce the computation cost, a considered heat sink is divided into 12 identical channels. Hence, computation domain is only $\frac{1}{12}$ of the heat sink. The computation domain, dimensions and its coordinate are depicted in Fig. 2. The domain is divided into three blocks: inlet block, heat sink block, and outlet block. The outlet block ($Lo$=50$d$) was included as domain in order to avoid the influence of the back flow stream in the final

results. A preliminary calculation, with whole heat sink treated as a computation domain, has been made. The results show that there is no significant difference of flow field and heat transfer characteristics for each channel.

The assumptions that have been made are: three-dimensional, laminar flow, incompressible, and steady state condition. Dissipation rate and buoyancy force are negligible. All of thermal and transport properties are constant. The walls, except the base of the heat sinks, are perfectly insulated. Heat transfer through the fins is a combination of conductive and convective heat transfer. Consequently, the present study is conjugate heat transfer problem.

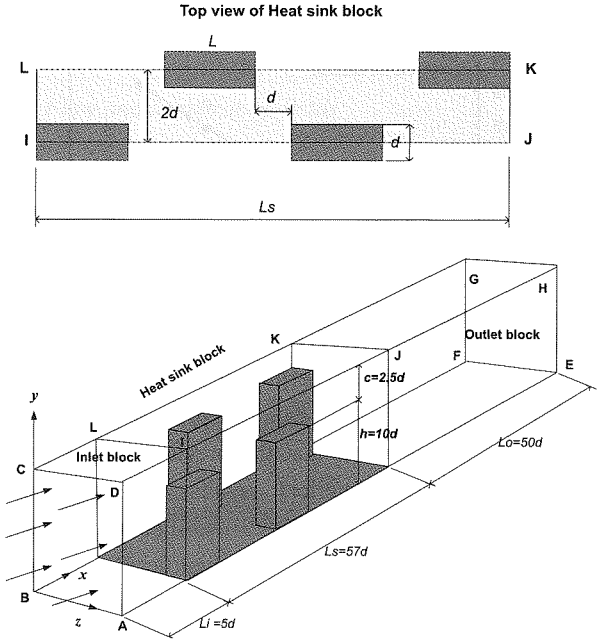


Fig. 2 The computation domain, dimensions and it's coordinate.

Based on the assumptions were made, the governing equations are as follows.

Continuity equation

$$\frac{\partial u_i}{\partial x_i} = 0 \tag{1}$$

Momentum equation:

$$\frac{\partial(\rho u_i u_j)}{\partial x_j} = -\frac{\partial p}{\partial x_j} + \frac{\partial}{\partial x_j}\left[\left(\mu \frac{\partial u_i}{\partial x_j} + \frac{\partial u_j}{\partial x_i}\right)\right] \tag{2}$$

Energy equations:

For fluid regions,

$$\frac{\partial(\rho c_p u_j T)}{\partial x_j} = \frac{\partial}{\partial x_j}\left[k \frac{\partial T}{\partial x_j}\right] \tag{3}$$

For solid regions,

$$\frac{\partial}{\partial x_j}\left[k \frac{\partial T}{\partial x_j}\right] = 0 \tag{4}$$

In the above equations, $u_i$ denotes the velocity components in Cartesian coordinate system with its direction $x_i$. $T$ denotes temperature and $P$ pressure.

*3.1 Boundary conditions*

For plane ABCD (inlet area): Uniform velocity in $x$-direction and constant temperature were applied.

$u = U_{in}$, $v$=0, $w$=0, and $T = T_\infty$ (5)

For planes ADEH and BCFG (symmetry surfaces): zero cross stream gradient conditions were applied.

$$\frac{\partial u}{\partial z} = \frac{\partial v}{\partial z} = \frac{\partial T}{\partial z} = 0 \text{ and } w = 0. \tag{6}$$

For planes ABFE and CDGH (solid surfaces): non-slip conditions for velocity components were specified.

$\frac{\partial T}{\partial y} = 0$, except for the base of the heat sink $T=T_b$ is specified (7)

For plane EFGH (outlet area): zero gradients for all variables were applied.

$$\frac{\partial u}{\partial x} = \frac{\partial v}{\partial x} = \frac{\partial w}{\partial x} = \frac{\partial T}{\partial x} = 0 \text{ and } P = P_\infty = 0 \tag{8}$$

*3.2 Computation code*

In order to solve the governing equations and boundary conditions a FORTRAN code program has been developed. The numerical solutions are explained as follows. All of the governing equations were discretized based via control volume approach on staggered grids system. To handle the convective terms, the power law scheme is used. In the momentum equations, the diffusion terms were calculated by using linear interpolation. In order to handle the abrupt changes in the thermal conductivity, in energy equation the diffusion terms were treated by using harmonic mean value. The sets of discreatized linear equations were solved by using SIP method proposed by Stone [10]. Velocity fields and pressure field were solved iteratively based on the

SIMPLE algorithm [11]. Iteration will be stopped if the normalized residuals less than $10^{-6}$.

*3.3 Comparison parameters*

In order to compare the performance of the heat sinks, the following parameters are used.

*3.3.1 Heat transfer coefficient*

Local heat transfer coefficient is defined by:

$$h = -k\partial T/\partial y\big|_{base} / (T_b - T_{av}) \quad (9)$$

where $T_{av}$ denotes average temperature of the fluids, and calculated by:

$$T_{av} = \sum uAT / \sum uA \quad (10)$$

Average local heat transfer as a function of its position from the inlet is calculated:

$$\bar{h}_x = \frac{1}{Lz}\sum h\,\partial z \quad (11)$$

In the above parameter, local heat transfer coefficient is only averaged in z-direction. Heat transfer coefficient of the heat sinks is defined by average local heat transfer coefficient of the wetted area, and calculated by:

$$\bar{h} = \frac{\sum -k\partial T/\partial y\big|_{sur} / (T_b - T_{av,x}) \times \partial A}{\sum \partial A} \quad (12)$$

*3.3.2 Total heat transfer rate*

Total heat transfer rate released by the heat sink is calculated by using two definitions. First: total heat rate absorbed by flowing air, it is calculated based on the temperature difference of the fluid at inlet and outlet area. Second: total heat rate released by base of the heat sink and it is calculated based on heat flux. Since the heat sink consists of 12 identical computation domains, the total heat transfer rate released by a heat sink is given:

$$Q_{tot} = 12\dot{m}c_p(T_{in} - T_{out}) \quad (13)$$

or

$$Q_{tot} = 12\sum k\partial T/\partial y\big|_{base} \times \Delta x \times \Delta z \quad (14)$$

*3.3.3 Pressure drop*

Since zero pressure is specified at the outlet area, the pressure drop is defined by the average pressure at the inlet area. The pressure drop is calculated by:

$$Pd = \tfrac{1}{A}\sum P\,\partial y\,\partial z\big|_{inlet} \quad (15)$$

*3.4 Validation of the code*

In order to make sure that the developed code is free of error coding and shows reasonable results, it was tested and verified extensively via comparing the results with the experiments [9]. A heat sink with continuous fins, similar to model HS1, at the same materials and dimensions was calculated using developed code. Dimensions of the tested heat sink are $W$=45 mm, length $Ls$=45 mm, $d$=1mm, $H_f$= 20 mm, number of continuous plates is 10. The average heat transfer coefficient and pressure drop of the heat sink are used as the comparison parameters. The pressure drop and heat transfer coefficient as a function of inlet velocity are presented in Fig. 3 and Fig. 4, respectively.

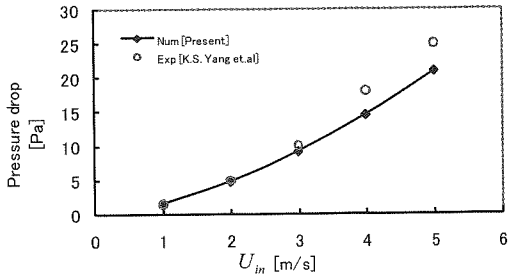


Fig. 3 Pressure drop as a function of inlet velocity from numerical and experimental results [9].

The figures show that the previous experimental and the presents numerical results do agree well, especially for velocity less than 3 m/s. For inlet velocity bigger than 3 m/s, the results show significant deviations. This is because for velocity bigger than 3 m/s the flow becomes turbulent. The developed code can not predict turbulent results well, because it was developed for laminar flow only. Since the present inlet velocity was less than 3 m/s, it can be said that the developed code reveals the satisfactory results. Based on this validation test, the developed code is ready to be used.

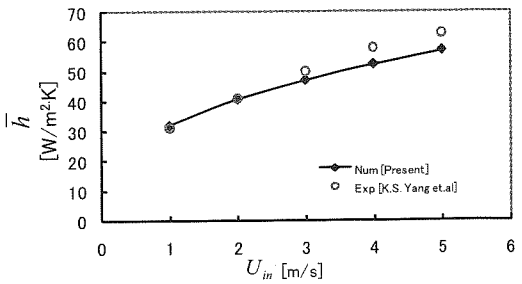


Fig. 4 Heat transfer coefficient as a function of inlet velocity from numerical and experimental results [9].

## 4. Results and Discussions

In order to understand flow field and heat transfer characteristics of this problem the numerical simulations have been carried out. As mentioned before, the fin number for each channel was varied, $n$=1, 4, 8, 16, 20, 25, and 29 and the inlet velocity was from $U_{in}$ = 0.5, 1, 2, and 3 m/s. Thus, the cases considered were 28 all together. The results will be divided and discussed in four groups. The streamlines, velocity vector, and temperature fields will be first discussed. The second is the average local heat transfer coefficient of the heat sinks. The third discussion will be the performance of the heat sinks as a function of inlet velocity and fan power input. The last discussion will be determining of optimum fin number for maximum heat transfer rate.

### *4.1 Flow and temperature fields*

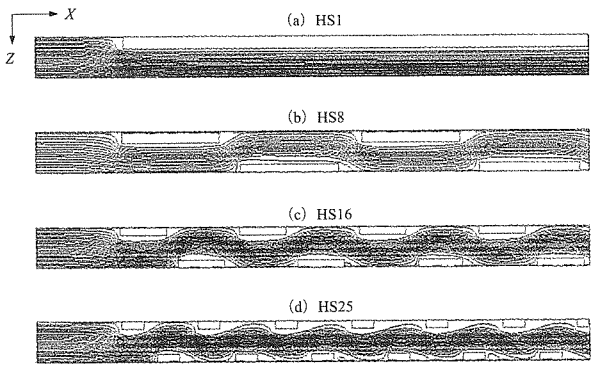


Fig. 5 Streamline patterns in the plane $y$ =12.5 mm (middle) from $x$=0 to $x$= 67 mm (a half of the heat sink) for inlet velocity 1 m/s.

Since the problem is three-dimensional, there are many planes of flow and temperature fields can be presented. For brevity, the flow and temperature fields of the middle plane for inlet velocity of 1 m/s are only presented. The typical streamlines of model HS1, HS8, HS16 and HS25 for plane which passes through half of the duct ($y$=12.5mm) are presented in Fig.5. The figure shows that for model HS1, there is no abrupt change of the streamlines due to continuousness of the fin. The flow reveals small acceleration at entrance, known as developing flow region. Then, it reaches fully developed flow region for the rest of the fin.

The different patterns are shown by model HS8, HS16, and HS25. In these models, offset strip fins postpone the flow to reach its fully developed region. Furthermore, the comparison of strip fins type (model HS8 and HS16) with pin fins type (HS25) shows a clear difference. For model HS8 and HS16, streamlines fill almost all areas around the fins. The strip fins lead the main stream to flow through all fluids areas of the computation domains. In these models, the presence of the reversal flows is not significant. This is because only a small reversal flow was observed in the rear of the fins. On the other hand, the streamlines of model HS25 shows that the main stream tends to flow only through the core. Compared to the strip fins type, the streamlines become more packed in the core but they become more diminished in areas between in a row fins. Hence, the presence of the reversal flows becomes significant. These facts can be seen clearly by observing velocity vector in the next paragraph.

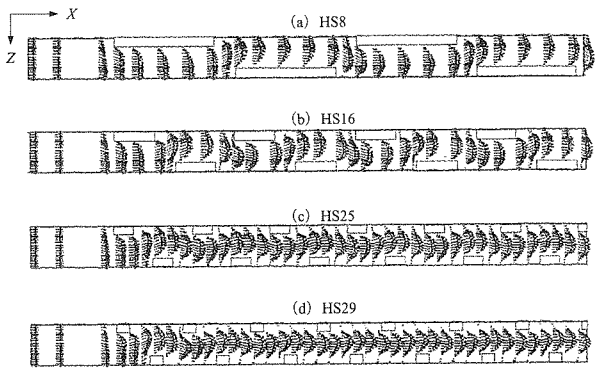


Fig. 6 Velocity vector in the plane $y$=12.5 mm (middle) from $x$=0 to $x$= 67 mm (a half of the heat sink) for inlet velocity 1 m/s.

Typical velocity vector for model HS8, HS16, HS25 and model HS29 for plane which passes through half of the duct ($y$=12.5mm) for inlet velocity 1 m/s are presented in Fig.6. In order to make clear the differences of the flow behaviors resulted by strip fins types and pin fins types, model HS8 and HS16 (on behalf of strip fins) and model HS25 and HS29 (on behalf of pin fins) have been chosen to be observed. For model HS8 and HS16, the area between in a row fins is wide enough to make the main stream to flow in this area. Indeed, only a small reversal flow behind the fins was observed. Hence, in comparison with area of the flowing fluids, the presence of the reversal flows is not significant.

For model HS25 and HS29, the main stream flows

through the core of the channel only. The areas between in a row fins are totally filled by reversal flows and/or stagnant fluids. The reversal flow starts from the rear surface of a fin and it ends at the front surface of another fin. Hence, the presence of the reversal flows will be significant. These results have been expected, if the fin number is too big the main stream will flow only through the core, while areas between in a row fins will be dominated by reversal flow. Since the main stream is concentrated in the core region, velocity gradient adjacent to both sides of the fins becomes bigger. However, velocity gradient adjacent to front and rear of the fins becomes smaller or almost zero. Vector velocity fields of HS25 and HS29 show these facts clearly. The effects of employing too big fin number will be further discussed in the heat transfer coefficient discussion.

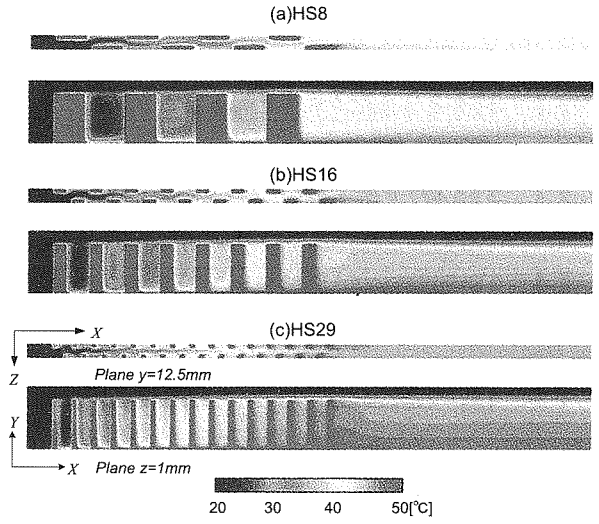


Fig. 7 Temperature fields along the computation domain for inlet velocity = 1 m/s.

Typical temperature fields of model HS8, HS16, and HS29 for inlet velocity 1m/s are shown in Fig.7. In the figure plane $x$-$z$ ($y$=12.5 mm) and plane $x$-$y$ ($z$=1 mm) are only presented. One should note that in comparison with strip fins, the cross-sectional area of the pin fins is smaller. Since the thermal conductivity of the fins is not infinity, for the same base temperature and the same heat transfer rate, temperature variation along pin fins will be less uniform than strip fins. This can be seen clearly by observing Fig. 7. For model HS8, temperature variation along the fins is almost uniform and equal to base temperature of the heat sink. This is because the cross-sectional area of the fins is sufficiently wide.

For model HS16, temperature variation along the fins becomes less uniform, especially for fins near to the inlet. This is caused by two reasons. First, the cross-sectional area of the fins becomes smaller. Second, the heat transfer coefficient of fin surfaces becomes bigger due to a bigger velocity gradient of the fluid adjacent to both fins sides. The effects of employing too big fin number can be seen clearly by observing model HS29, the most not uniform temperature variation along the fins. This model has the smallest cross-sectional area of the fins. Because of this, the pin fins will not be able to supply an adequate amount of heat transfer rate. Hence, the temperature variation along the fins will change abruptly. Since the heat transfer coefficient of fins at location near the inlet is relatively bigger than fins at location farther at downstream, the temperature variations along fins near the inlet will be bigger. This can be seen clearly by observing temperature field of model HS29 in Fig. 7 (c).

### *4.2 Heat transfer coefficient*

The next discussion is average local heat transfer coefficient of the base of the heat sink as a function of its position from the inlet. This parameter is given in equation (11). In the simple word, this parameter can be viewed as the ability of the base of the heat sinks to transfer the heat into the flowing air. One should note that some parts of the base, where the fins are attached, will give heat transfer coefficient relatively bigger than the other parts without any fins. This is because the presence of the extended surfaces provided by the fins. The average local heat transfer coefficient for model HS1, HS8, HS16, and HS29 are presented in Fig. 8.

For model HS1 (heat sink with continuous fins), in the figure shown by black dashed line, the heat transfer coefficient is relatively big in the front region (developing flow or boundary layers region) and suddenly decrease to reach its fully developed region at locations farther downstream. For model HS8, in the figure shown by black solid line, the presence of the offset strip fins prevents the line to reach its fully developed flow region. This results in a very significant heat transfer enhancement. The only weakness is the presence of the gaps between strip fins. These gaps result in a very low heat transfer coefficient due to absence of extended surface. The effect of these gaps to the total heat transfer rate can't be examined by observing Fig. 8, it will be discussed later.

For model HS16, in the figure shown by red dashed line, strip fins show their superior. This line, except the gaps, shows that the strip fins of model HS16 keep the heat transfer coefficient higher than model HS8. This is because the velocity gradient of model HS16 is relatively bigger than model HS8. Furthermore, cross-sectional area of the fins in model HS16 is sufficiently enough to support heat transfer rate. For model HS29, the average local heat transfer coefficient is shown by blue solid line. Comparison of model HS8 with model HS29 reveals that model HS8 is superior to HS29 in the entrance region only, but inferior for the rest region. For fins at location near the inlet, heat transfer coefficient for model HS29 is relatively bigger than model HS8. This is because velocity vector of model HS29 is relatively bigger than model HS8. However, for fins at location further downstream in fully developed flow region, heat transfer coefficient of model HS29 is lower than HS8. This is because the presence of the reversal flow becomes significant in model HS29. In this model, the areas between in a row fins are filled by reversal or stagnant flow. Because of this heat transfer coefficient from front and rear surfaces of the fins becomes weak.

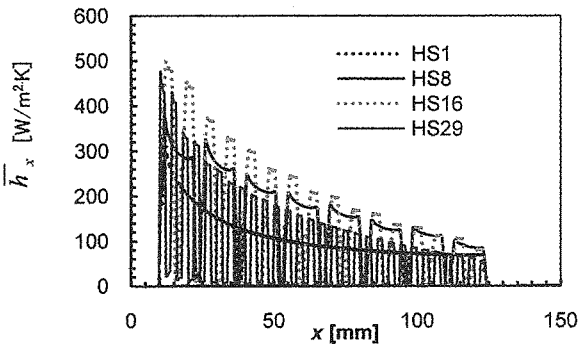


Fig. 8 Average local heat transfer coefficient for inlet velocity = 1 m/s

The comparison of model HS29 with HS16 shows that model HS16 is superior to HS29 for all fins, even though for fins at location near the inlet. It is true that for fins at location near the inlet, model HS29 is supposed to be superior to model HS16 due to a bigger velocity gradient. However, since the cross-sectional area of the pin fins of model HS29 is too small and it will not be able to supply the higher heat transfer rate, the fins near the inlet have failed to take this advantage. For fins at location further downstream, both areas adjacent to front and rear surfaces of the fins are filled by reversal or dead flow. Because of this, the average local heat transfer coefficient of model HS29 is always smaller than model HS16.

### *4.3 Performance of the heat sink*

In this study, performance of the sinks is examined by using total heat transfer rate as a function of inlet velocity and fan power input. The effect of quantity of the gaps in the previous section will be examined here by observing models with big fin number. The total heat transfer rate as a function of velocity is depicted in Fig. 9. The horizontal axis is inlet velocity and vertical is total heat transfer rate. As expected, the heat transfer rate increases as the inlet velocity increases. The figure shows that attaching offset strip fins or pin fins instead of continuous fins do enhance the heat transfer rate. It also shown that varying $n$ from 1 to 4 (model HS1 to model HS4) means enhancing heat transfer rate very significant, averagely almost two times. The same effect also resulted by varying fin number from 4 to 8 (model HS4 to model HS8) and also from model HS8 to model HS16. However the rate of enhancement decreases as fin number increases. Even though it becomes very small, enhancement can be resulted from 16 to 20 (model HS16 to model HS20).

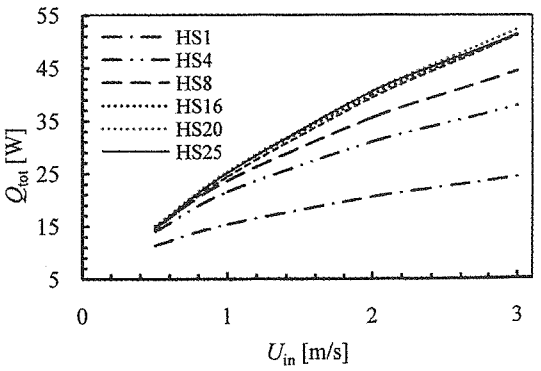


Fig.9 Total heat transfer rate as a function of inlet velocity

However, for $n$ more than 20 the enhancement seems to be stagnant or negative. This can be seen clearly by observing model HS20, HS25, and HS 29. This fact has been predicted in the previous section. If fin number is too big the following effects will be appeared. The cross-sectional area of the fins becomes smaller, the presence of the reversal flow becomes significant and number of fins at locations in fully developed flow

regions becomes larger. These effects, simultaneously, will reduce the total heat transfer rate. These results do agree with [12], it says flow over a tube banks with more than 16 rows is considered to be fully developed, hence no further substantial changes in the flow and temperature fields. The conclusion can be drawn that there exist an optimum fin number for maximum heat transfer rate.

Pressure drop as a function of inlet velocity for all models is presented in Fig.10. The figure shows that pressure drop increases with the rise of the inlet velocity. As expected that the pressure drop for continuous fins, model HS1, is the lowest. This is because the continuous fins give the smallest flow resistance. It can be seen that pressure drop increases with the rise of fin number. Heat sinks with bigger fin number result bigger velocity gradient due to the presence of the reversal flow. The bigger velocity gradient results the bigger pressure drop. Based on this fact, model HS29 results the biggest pressure drop, followed by model HS25.

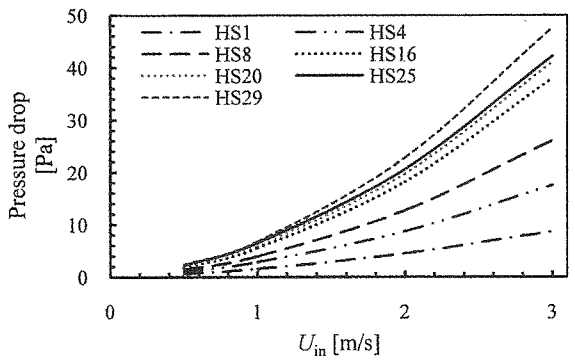


Fig. 10 Pressure drop as a function of inlet velocity

*4.4 Optimum fin number*

As mentioned before that the objective of this study is to show that there exist an optimum fin number for maximum heat transfer rate. Based on the previous discussions, the objective has been shown. In order to make a clear examination, total heat transfer rate as a function of fin number is presented in Fig. 11. The figure shows that for the considered heat sinks and their dimensions with the given range of inlet velocity the optimum fin number is 20. Attaching offset fin number more than or less than 20 will decrease the heat transfer rate.

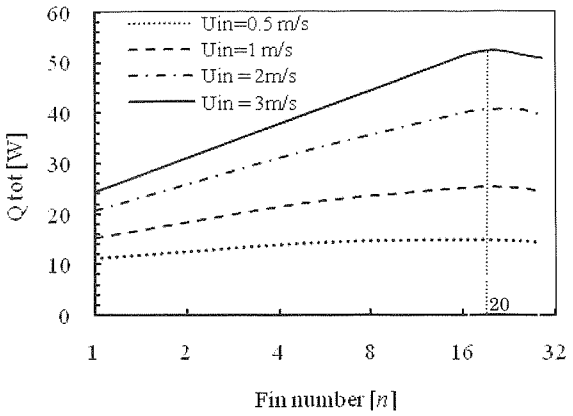


Fig. 11 Total heat transfer as a function of fin number

## 5 Conclusions

Flow field and heat transfer characteristics of heat sinks with continuous, offset strip or pin fins have been studied numerically. The conclusions are as follows.

1. Attaching offset strip or pin fins with staggered arrangement instead of continuous fins does enhance the heat transfer rate. This is because the presence of the offset strip/pin fins postpones the flow field to reach its fully developed flow region.
2. However, in comparison with less fin number, attaching too many fin number will decrease the heat transfer rate. This is because the cross-sectional area of the fins becomes smaller, the presence of the reversal flow becomes significant and number of fins at locations in fully developed flow region becomes larger.
3. It was shown that there exists an optimum fin number for maximum heat transfer rate.
4. For the considered heat sinks with their dimensions, materials and operational conditions the optimum fin number was 20.
5. Attaching the optimum fin number, $n$=20, the heat transfer rate will be enhanced up to 214 percent, on the other hand, total mass of the fins material will be reduced up to 66.6 percent in comparison with a heat sink with continuous fins at inlet velocity $U_{in}$=3 m/s.

One should note that the optimum fin number resulted in here is restricted for the considered heat sinks, their dimensions, materials, and operational conditions. This study was aimed to show that employing strip fins instead of continuous fins does enhance the heat transfer rate. However, there exists a limit of employing offset

strip fins. This has been shown in the present paper.

## References


[1] M. Iyengar and A. Bar-Cohen, "Design for manufacturability of SISE parallel-plate forced convection heat sinks," IEEE Trans. Comp. Packaging Technol., 24 (2001) 150-158.

[2] S. Naik, S. D. Probert, and I. G, "Heat transfer characteristics of shrouded longitudinal ribs in turbulent forced convection," Int. J. Heat Fluid Flow., 20 (1999) 374-384.

[3] N. Sahiti, A. Lemouedda, D. Stojkovic, F. Durst, and E. Franz, "Performance comparison of pin fin in-duct flow arrays with various pin cross-sections," App. Therm. Eng. 26 (2006) 1176-1192.

[4] O. N. Sara, S. Yapici, and M. Yilmaz, "Second law analysis of rectangular channels with square pin-fins," Int. Comm. Heat Mass Transfer 28 (2001) 617-630.

[5] Z. Chen, Q. Li, D. Meier, and H.-J. Warnecke, "Convective heat transfer and pressure loss in rectangular duct with drop-shaped pin fins," Heat Mass Transfer 33 (1997) 219-224.

[6] Q. Li, Zh. Chen, U. Fletcher, and H.-J. Warnecke, "Heat transfer and pressure drop characteristics in rectangular channels with elliptic pin fin," Int. J. Heat Fluid Flow 19 (1998) 245-250.

[7] O. Leon, G. D. Mey, and E. Dick, "Study of the optimal layout of cooling fins in forced convection cooling," Microelectronics Reliability 42 (2002) 1101-1111.

[8] K. Al-Jamal and H. Khashasneh, "Experimental investigation in heat transfer of triangular and fin fin arrays," Heat Mass Transfer 34 (1998) 159-162.

[9] K. -S. Yang, W. -H. Chu, Ing,-Y. Chen, and C.-C Wang, "A comparative study of the airside performance of heat sinks having pin fin configurations", Int. J. Heat Mass Transfer (2007), doi:10. 1061/i.ijheatmasstransfer.2007.03.006.

[10] H. L. Stone, "Iterative solution of implicit approximations of multidimensional partial differential equations", SIAM J. Num. Anal 5 (1968) 530-558.

[11] S. V. Patankar, Numerical Heat Transfer and Fluid Flow, Hemisphere, Washington, DC, 1980.

[12] A. Zukauskas, Heat transfer from tubes in cross flow, in: J. P. Harnet, Th. F. Irvine (Eds.), Advances in Heat Transfer, vol. 18, Academic Press, New York, 1987.


## Nomenclature

| | |
|---|---|
| $A$ | : Surface area |
| $c_p$ | : specific heat |
| $d$ | : fin thickness |
| $h$ | : heat transfer coefficient |
| $H_f$ | : fin height |
| $k$ | : thermal conductivity |
| $L$ | : fin length |
| $Lz$ | : length in z-direction |
| $Ls$ | : length of the heat sinks |
| $m$ | : mass |
| $\dot{m}$ | : mass flow rate |
| $n$ | : fin number for each channel |
| $P$ | : Pressure |
| $Pd$ | : Pressure drop |
| $Q$ | : total heat transfer rate |
| $T$ | : Temperature |
| $u, v, w$ | : velocity components |
| $\dot{V}$ | : volume rate |
| $W$ | : width of the heat sink |
| $x,y,z$ | : Cartesian coordinate |

*Greek symbol*

| | |
|---|---|
| $\mu$ | : dynamic viscosity |
| $\rho$ | : density |
| $\infty$ | : related to ambient |

*Subscript*

| | |
|---|---|
| $av$ | : related to average |
| $b$ | : related to base of the heat sinks |
| $f$ | : related to fin |
| $in$ | : related to inlet |
| $out$ | : related to outlet |
| $tot$ | : related to total |